10.1071/CH20169_AC

Australian Journal of Chemistry 2020, 73(12), 1226-1236

Supplementary Material

Bismuth(III) Thiophosphinates: Understanding How Small Atomic Change Influences Antibacterial Activity and Mammalian Cell Viability

Dimuthu C. Senevirathna,[A] Rebekah N. Duffin,[A,B] Liam J. Stephens,[A] Megan E. Herdman,[A] Melissa V. Werrett,[A,C] and Philip C. Andrews[A,C]

[A]School of Chemistry, Monash University, Clayton, Vic. 3800, Australia.

[B]Current address: Drug Delivery, Disposition and Dynamics, Monash Institute of Pharmaceutical Sciences, Parkville, Vic. 3052, Australia.

[C]Corresponding authors. Email: melissa.werrett@monash.edu; phil.andrews@monash.edu

<u>Content</u>

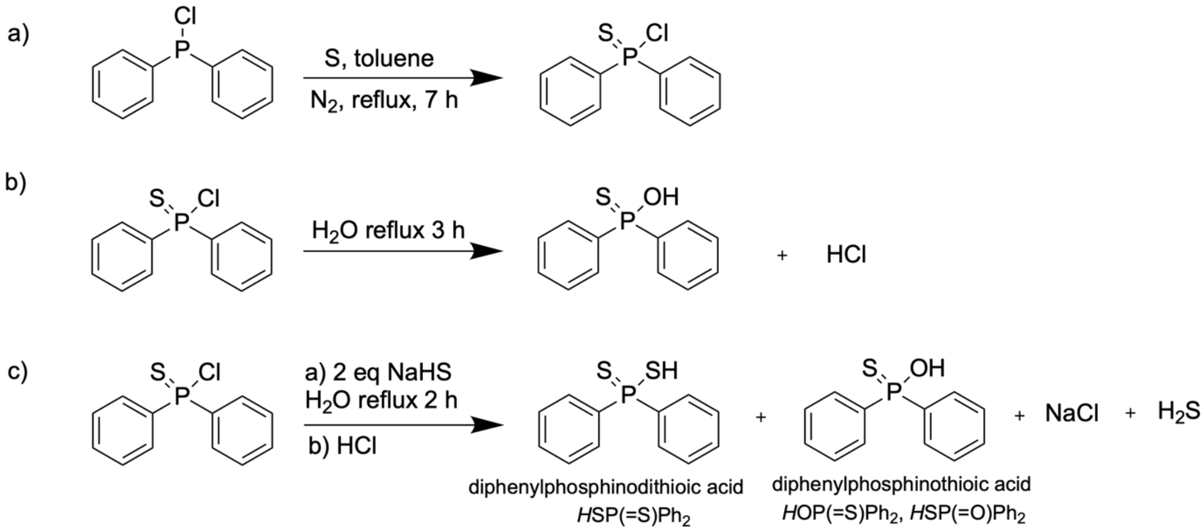

Scheme S1. Synthesis of diphenylphosphinothioic acid, *H*OP(=S)Ph_2/*H*SP(=O)Ph_2 and diphenylphosphinodithioic acid, *H*SP(=S)Ph_2.

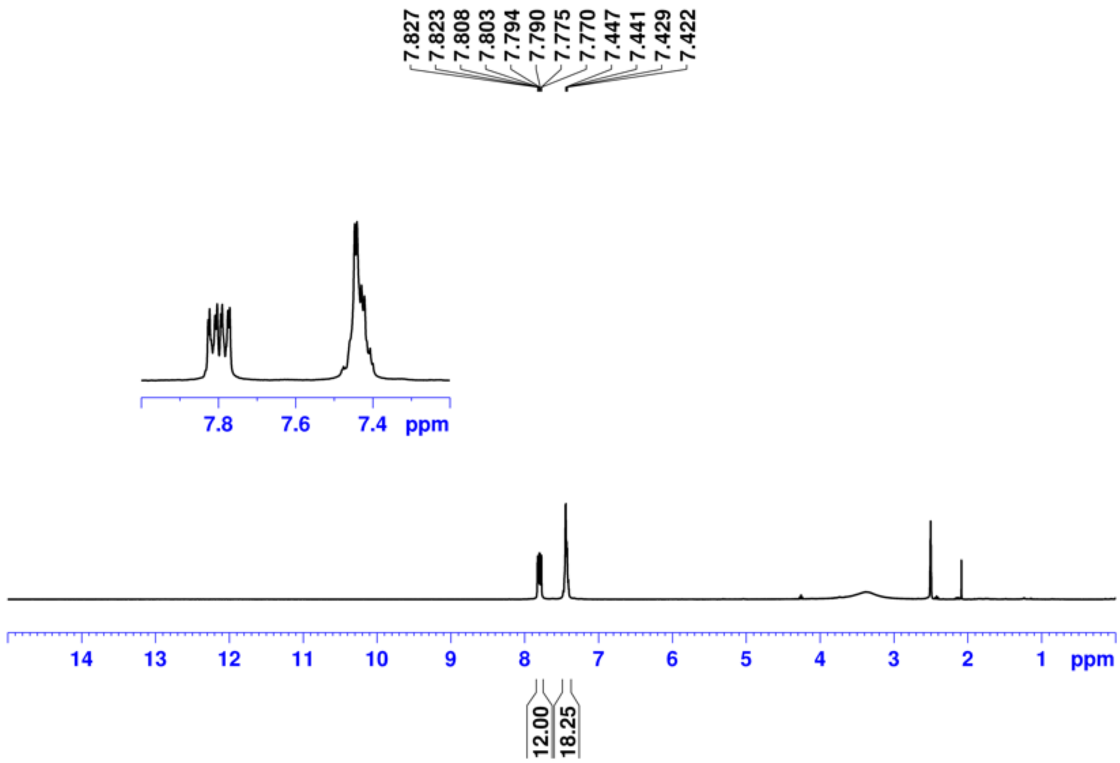

Fig. S1. ^{1}H NMR of $[Bi(SP(=O)Ph_2)_3]$ (**1**) in DMSO-d_6.

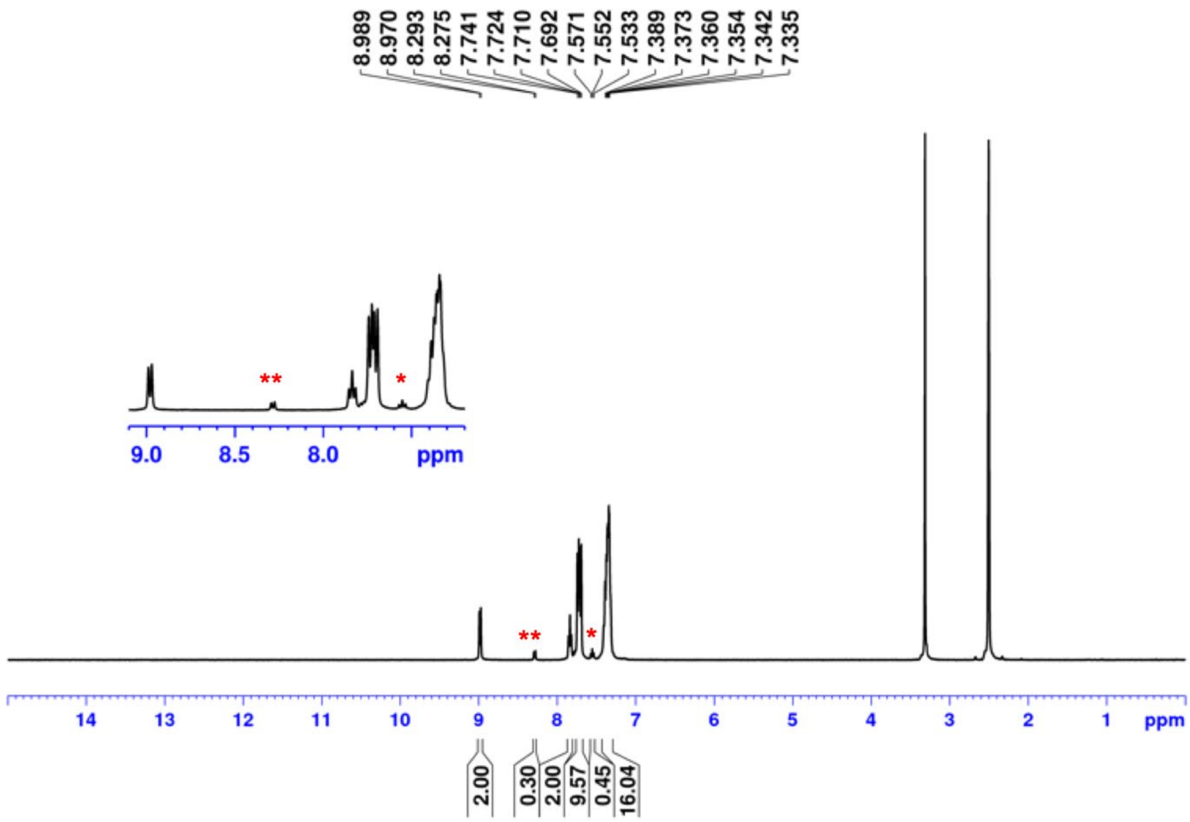

Fig. S2. ^{1}H NMR of $[BiPh(SP(=O)Ph_2)_2]$, (**2**) in DMSO-d_6. **ortho and *meta Bi-**Ph** protons from complex **3**.

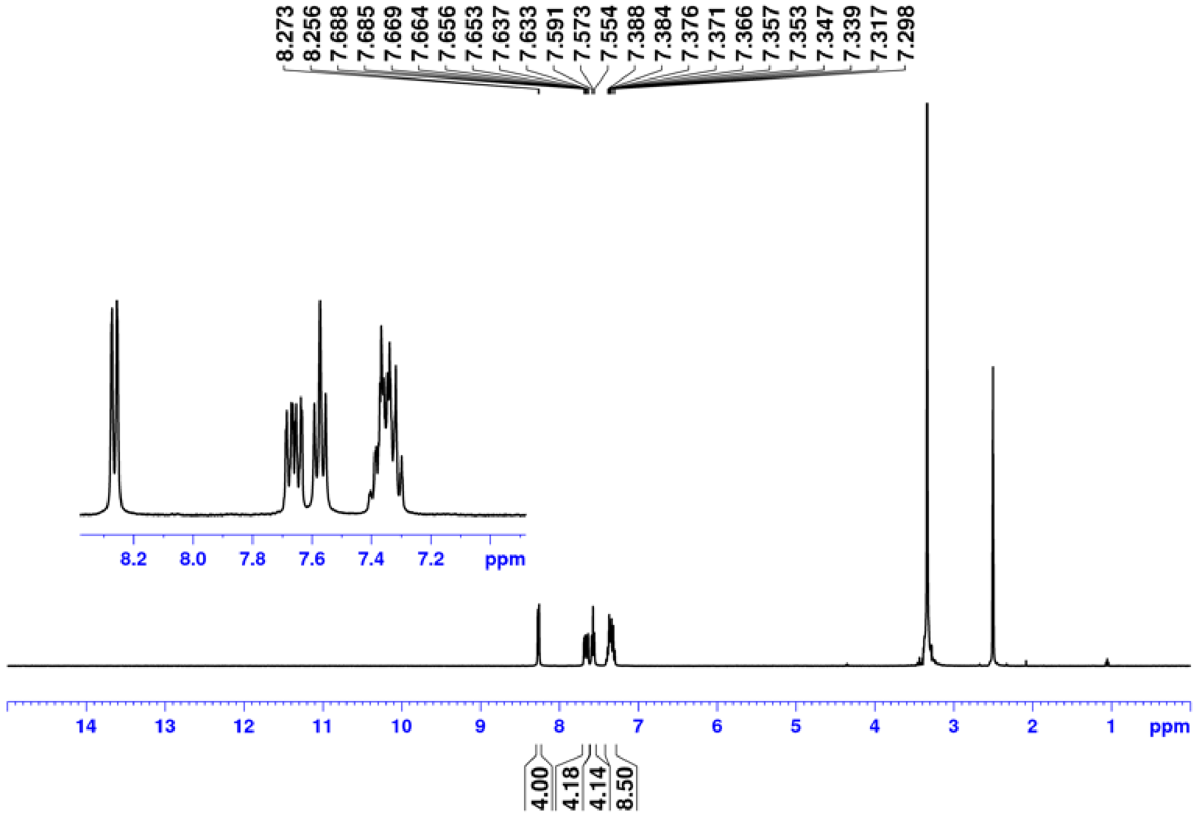

Fig. S3. ^{1}H NMR of [$BiPh_2(SP(=O)Ph_2)$] (**3**) in DMSO-d_6.

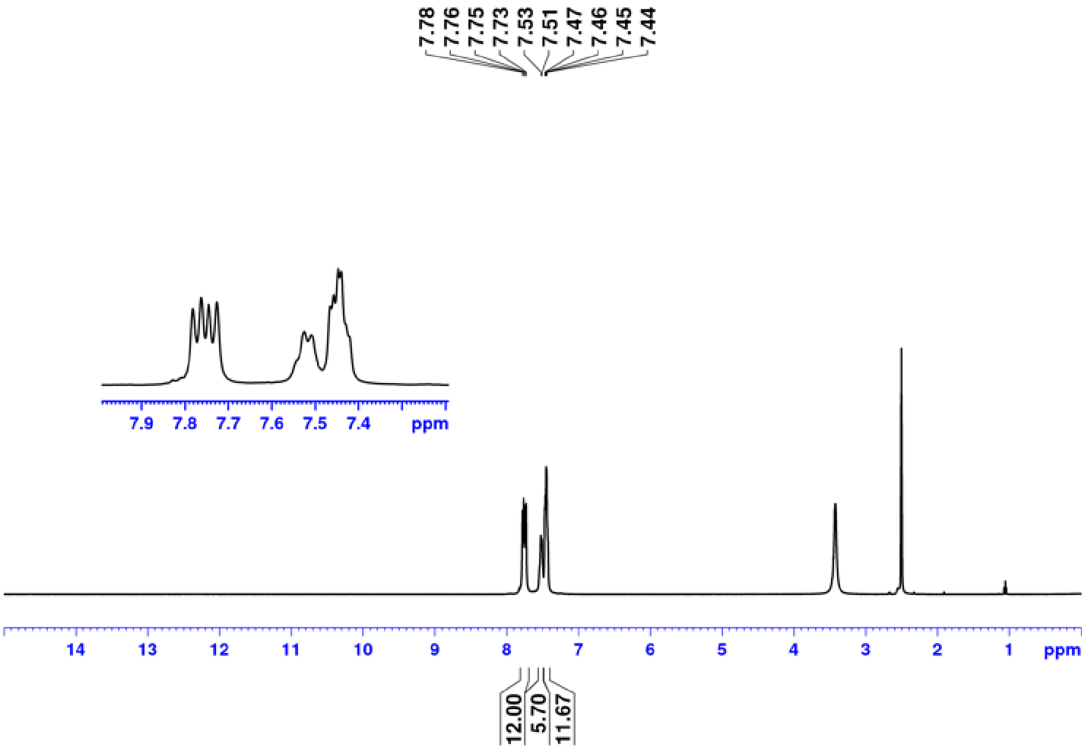

Fig. S4. ^{1}H NMR of [$Bi(SP(=S)Ph_2)_3$] (**4**) in DMSO-d_6.

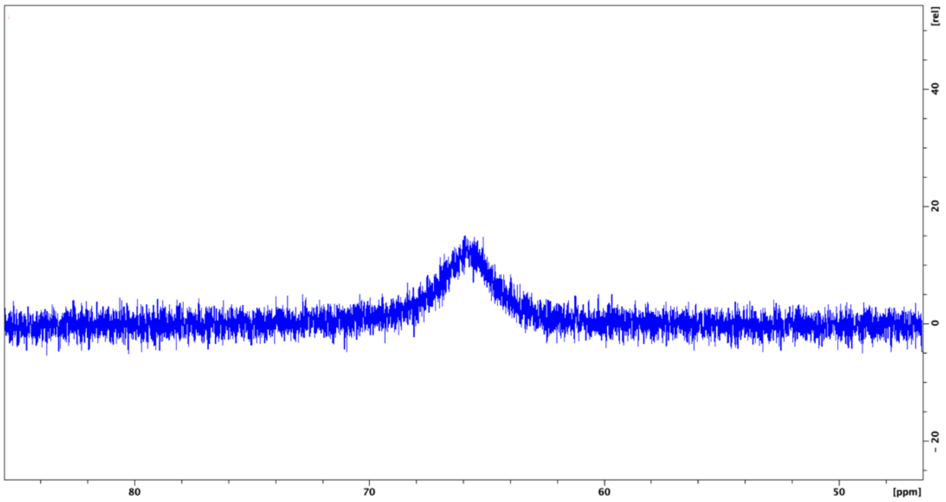

Fig. S5. ^{31}P NMR of $[Bi(SP(=O)Ph_2)_3]$ (**1**) in DMSO-d_6.

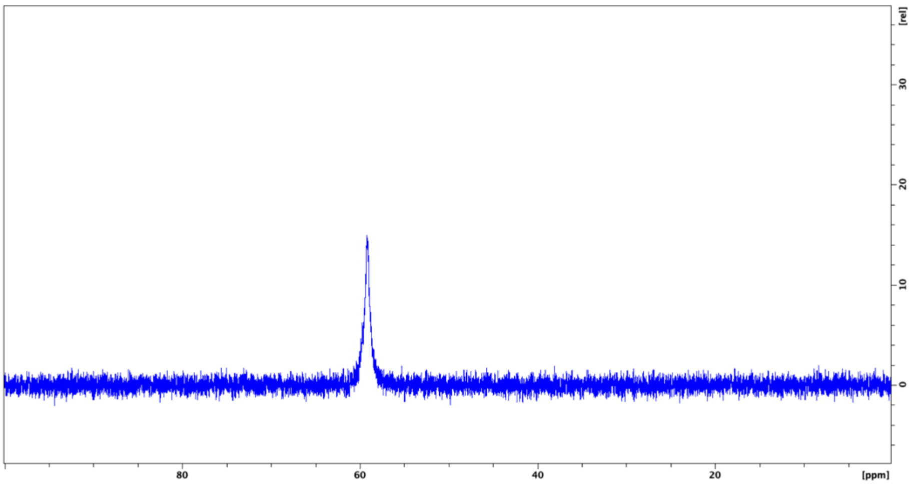

Fig. S6. ^{31}P NMR of $[BiPh(SP(=O)Ph_2)_2]$ (**2**) in DMSO-d_6.

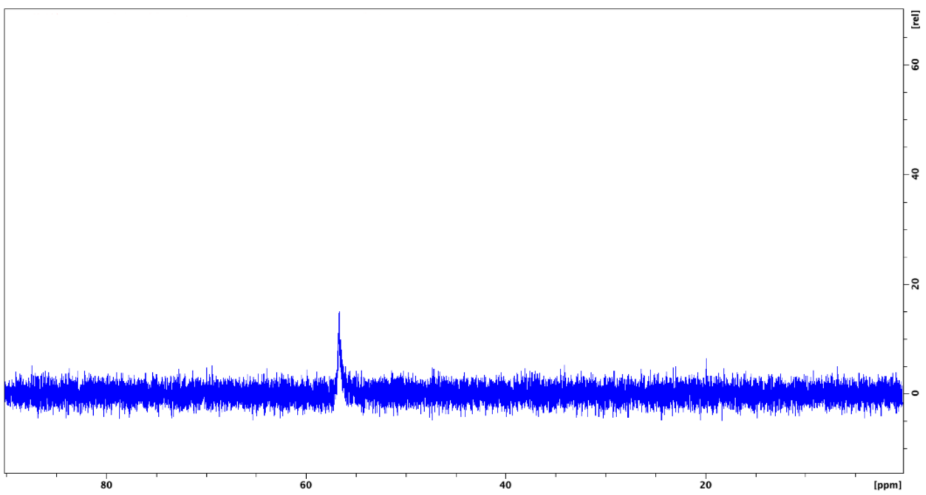

Fig. S7. ^{31}P NMR of $[BiPh_2(SP(=O)Ph_2)]$ (**3**) in DMSO-d_6.

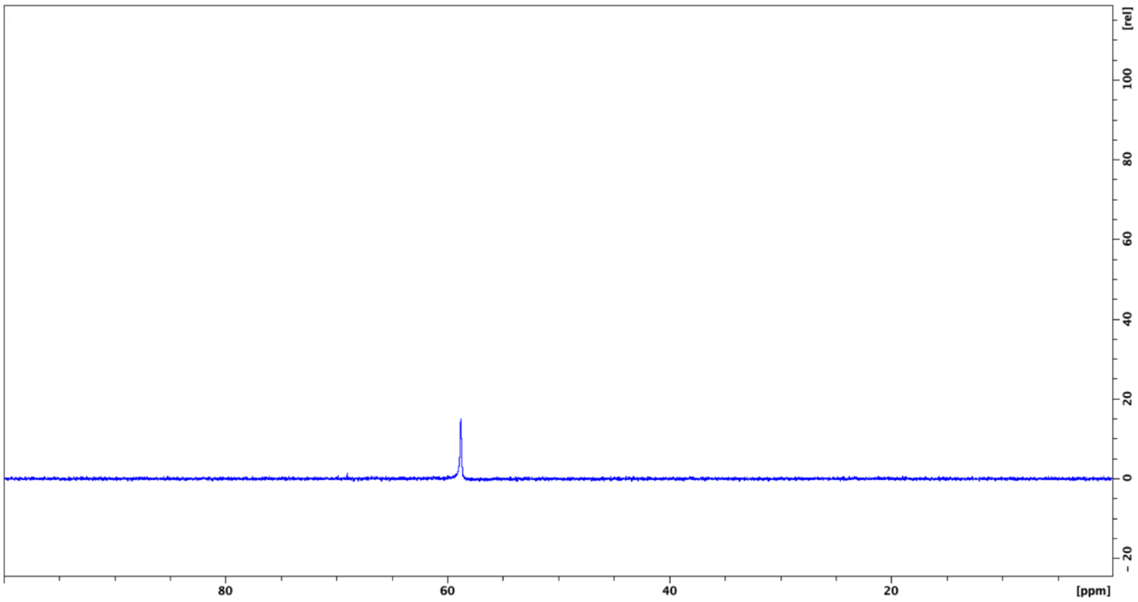

Fig. S8. ^{31}P NMR of [Bi(SP(=S)Ph$_2$)$_3$·DMSO] (**4**) in DMSO-d$_6$.

Table S1. Crystallographic data and structure refinement for complexes **2**, **3** and **4**. CCDC numbers 1947001-1947003.

	2	**3**	**4**·DMSO
Formula	$C_{30}H_{25}BiO_2P_2S_2$	$C_{24}H_{20}BiOPS$	$C_{38}H_{36}BiOP_3S_7$
M_r	752.54	596.41	1034.98
Crystal size [mm]	0.23 x 0.16 x 0.09	0.21 x 0.17 x 0.10	0.24 x 0.16 x 0.10
Crystal system	Monoclinic	Monoclinic	Monoclinic
Space group	*P2₁/c*	*P2₁/n*	*P2₁/n*
a [Å]	10.7908(4)	9.6557(4)	9.29900(10)
b [Å]	11.0293(4)	10.5962(4)	21.7360(2)
c [Å]	23.3960(6)	21.2320(9)	20.4159(2)
α [°]	90	90	90
β [°]	94.434(2)	93.243(3)	100.7700(10)
γ [°]	90	90	90
V [Å^3]	2776.14(16)	2168.85(15)	4053.84(7)
Z	4	4	4
T [K]	123(2)	123(2)	123(2)
$\rho_{calcd.}$ [g cm^{-1}]	1.801	1.827	1.696
μ [mm^{-1}]	15.175	8.311	13.269
Independent reflections collected	5740	6685	8349
R_{int}	0.1301	0.0548	0.0473
$R1$ [$I > 2\sigma(I)$]	0.0587	0.0261	0.0281
$wR2$ (all data)	0.1611	0.0486	0.0733
GoF	1.015	1.009	1.095

PXRD Study

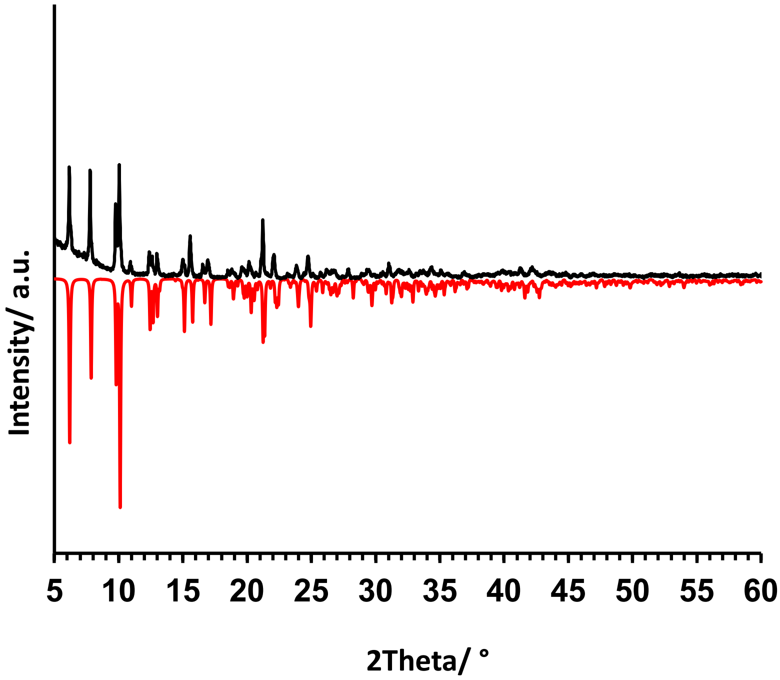

Fig. S9. Comparison of the powder X-ray diffraction pattern of bulk crystalline product (black, top) and the calculated pattern from the single crystal X-ray diffraction studies (red, bottom) of [BiPh(SP(=O)Ph_2)$_2$] (**2**).

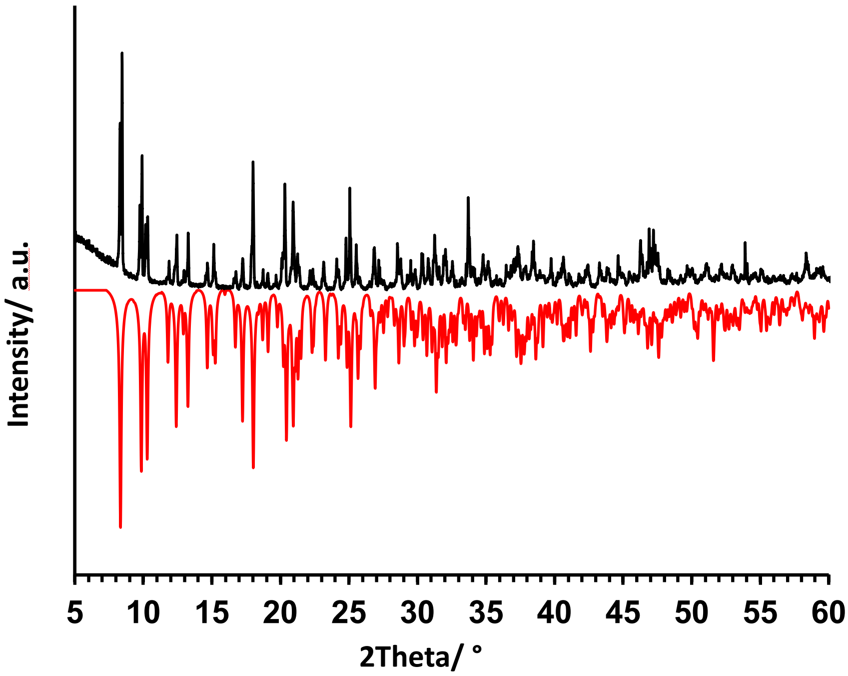

Fig. S10. Comparison of the powder X-ray diffraction pattern of bulk crystalline product (black, top) and the calculated pattern from the single crystal X-ray diffraction studies (red, bottom) of [$BiPh_2$(SP(=O)Ph_2)] (**3**).

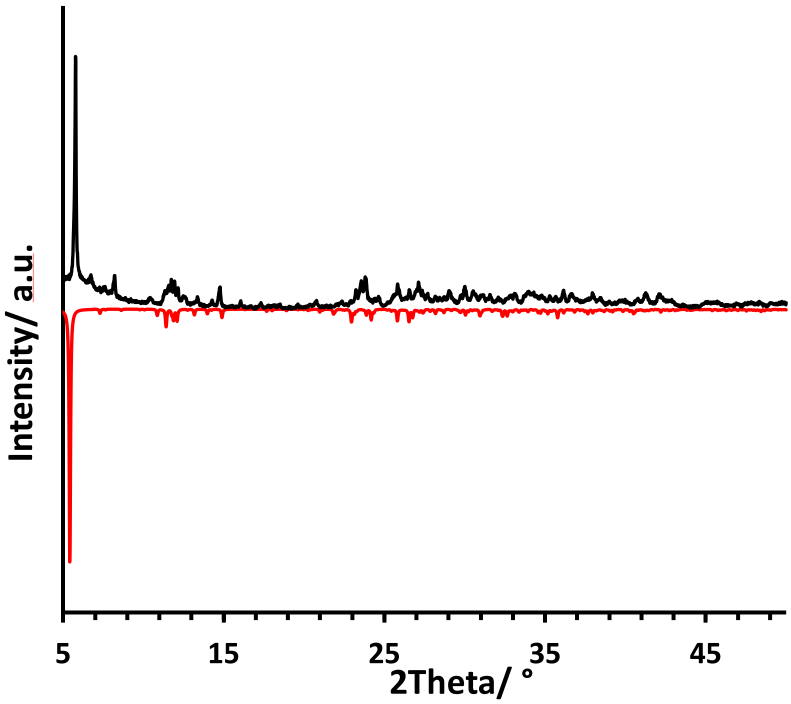

Fig. S11. Comparison of the powder X-ray diffraction pattern of bulk crystalline product (black, top) and the calculated pattern from the single crystal X-ray diffraction studies (red, bottom) of $[Bi(SP(=S)Ph_2)_3{\cdot}DMSO]$ (**4**).

Table S2: Selectivity indices of compounds **1** – **4,** where SI = IC_{50} / MIC. IC_{50} of complexes against human fibroblast cells.

Compound	*MRSA*	*VRE*	*E. coli*	*P. aeruginosa*
1 $[Bi(SP(=O)Ph_2)_3]$	/	/	/	/
2 $[BiPh(SP(=O)Ph_2)_2]$	9.2	9.2	2.3	1.1
3 $[BiPh_2(SP(=O)Ph_2)]$	2.5	2.5	1.3	0.30
4 $[Bi(SP(=S)Ph_2)_3]$	0.49	0.49	/	/